ACP
AMERICAN COLLEGE OF PROSTHODONTISTS®

Biomechanical Evaluation of Tooth- and Implant-Supported Fixed Dental Prostheses with Various Nonrigid Connector Positions: A Finite Element Analysis

Tuncer Burak Özcelik, DDS, PhD,[1] Ersan Ersoy, DDS, PhD,[2] & Burak Yilmaz, DDS, PhD[3]

[1] Department of Prosthodontics, Başkent University, Adana, Turkey
[2] Department of Prosthodontics, Ankara University Faculty of Dentistry, Ankara, Turkey
[3] Division of Restorative Dentistry and Prosthodontics, The Ohio State University College of Dentistry, Columbus, OH

Keywords
Implant; finite element method.

Correspondence
Burak Yilmaz, Division of Restorative and Prosthetic Dentistry, The Ohio State University College of Dentistry, Room 3005A Postle Hall, 305 West 12th Ave., Columbus, OH 43210-1267.
E-mail: yilmaz.16@osu.edu

Accepted January 30, 2010

doi: 10.1111/j.1532-849X.2010.00654.x

Abstract

Purpose: In the tooth- and implant-supported fixed dental prosthesis (FDP), rigid and nonrigid connector (NRC) designs have been preferred by clinicians for many years. The aim of this study was to analyze the stress distribution on the connecting areas of the superstructure and supporting structure of the tooth- and implant-supported FDP designs under both static vertical and oblique occlusal loads.
Materials and Methods: Four 2D finite element analysis (FEA) models were prepared presuming that the first and second molars were missing, and that the implant (3.80-mm diameter × 13-mm length) was placed in the second molar NRC design and patrix-matrix position supported by teeth/implants. Nonlinear contact elements were used to simulate a realistic interface fixation within the implant system and the sliding function of the NRC. Supporting periodontal ligament and alveolar bone (cortical and trabecular) were also modeled. Linear static analysis was performed on the prepared 2D solid models with a total masticatory force of 250 N (50 N for premolar, 100 N for first molar, 100 N for second molar), 0° (at a right angle) and 30° to the long axis of the supports. The maximum equivalent Von Mises (VM_{Max}) was analyzed around the supporting teeth/implant and connector areas on tooth- and implant-supported FDP.
Results: The simulated results indicated that the highest level of VM_{Max} (400.377 MPa) was observed on the NRC with the matrix positioned on the implant site of tooth- and implant-supported FDP under vertical occlusal load. The highest level of VM_{Max} (392.8 MPa) under oblique occlusal load was also observed on the same model; however, the lowest VM_{Max} value around implants was observed with the NRC when the patrix was positioned on the implant site of the FDP. Under vertical occlusal loads, in designs where the NRC was placed on the implant site, the stress formed around the implant decreased when compared to the designs where the NRCs were positioned on the tooth site.
Conclusions: The efficiency of the NRC exhibited varying behavior depending on the direction of the load applied. The use of the patrix part of the NRC on the implant site may be more efficient in reducing the stress formation around the implant.

Tooth and implant-supported fixed dental prosthesis (TIFP) is a treatment option for distal extension partially edentulous areas. Economic and anatomic considerations may sometimes limit the use of a second implant to provide completely implant-supported restorations. In such situations, the primary concern relates to the difference between the mobility of the natural tooth and the osseointegrated implant, which makes the biomechanical behavior of the entire system complicated.[1-3]

An osseointegrated implant is "rigidly" fixed to bone and may move only 10 μm, which is primarily a result of bone flexure, while a natural tooth with a healthy periodontal ligament has a mobility of 50 to 200 μm.[4-8] This movement disparity may cause relative motion of the implant and tooth superstructure when the splinted system is loaded.[4-10] During loading, the higher bending moment induced by the mismatch between the implant and tooth may result in abutment screw loosening (screw-retained) or fracture of the implant or prosthesis.[4-10] Loss of osseointegration and increased marginal bone resorption may also occur around the implant as a result of overload.[11-17]

When the connection of implants and teeth in the same prosthesis are treatment planned, there are two design options: a TIFP with a rigid connection (RC) or TIFP with a nonrigid connector (NRC). NRCs act as stress directors with the ability to separate the splinted units, thus in theory compensating for the variability in mobility between the implant and tooth.[1,2] However, several reports have explored the use of NRCs and the association with abutment tooth intrusion.

Controversial etiology for the phenomenon of tooth intrusion includes disuse atrophy, mechanical binding,[11] and impaired rebound memory.[13-15,18] Indeed, clinical observations have also cast doubt with respect to function, with most revealing nonsignificant or minimal differences between TIFP with RC and TIFP with NRCs.[19-23]

In contrast, TIFP with RC has been advocated by certain authors since the prosthesis and implant possess the inherent flexibility to accommodate dissimilar mobility characteristics;[24-29] however, the results of a long-term radiographic follow-up evaluation revealed more bone loss around TIFP with RC when compared to TIFP with NRC.[30] Accordingly, consensus regarding the proper connector design for TIFP has not been reached, and the issue remains controversial.

The results of previous in vitro studies are controversial as are in vivo studies where biomechanics have been investigated in terms of the use of NRCs in TIFP.[28,31-35] Although TIFPs are used as a treatment modality by clinicians in cases of partial edentulism, there remain a limited number of studies on the location of the NRC (site of the natural tooth or site of the implant) and their biomechanical effects on the TIFPs and particularly the positioning of the patrix and matrix parts.

The finite element method (FEM) provides mechanical responses and modifies parameters in a more controllable manner, driving its common use as an analytical tool in dental biomechanical studies.[28,31-36] Accordingly, the purpose of this study was to examine the stress distribution on the connecting areas of the superstructure (dental prostheses) and supporting structure of the TIFP designs under both static vertical and oblique occlusal loads with 2D FEM. Furthermore, the evaluation of location of NRCs and positioning of patrix and matrix parts were investigated.

Materials and methods

TIFP designs for a partially edentulous mandible with distal extension were investigated in this study. Four models, each with a different NRC location design, were prepared for 2D finite element analysis (FEA) (Table 1). It was presumed that first and second molars were missing in the 2D FEA models.

The outlines of dentine, pulp, prosthesis, and alveolar bone boundaries were created according to the literature.[37] The coordinates for each point on the boundaries were entered into the FE program (Marc K7.2/Mentat 2001; MARC Analysis Research Corporation, Palo Alto, CA) to generate areas of the tooth, prosthesis, and bone. Posterior mandibular ridge height was determined to be 23 mm, cortical bone thickness as 1.5 mm, and the periodontal membrane width was accepted as 0.2 mm (Fig 1).

Table 1 Four tooth-implant-supported fixed prosthesis designs, each with a different NRC location

	Tooth-implant-supported fixed prosthesis designs
Model MDP	Second premolar and implant connected by nonrigid connector with matrix positioned on distal surface of second premolar
Model PDP	Second premolar and implant connected by nonrigid connector with patrix positioned on distal surface of second premolar
Model MMI	Second premolar and implant connected by nonrigid connector with matrix positioned on mesial surface of implant
Model PMI	Second premolar and implant connected by nonrigid connector with patrix positioned on mesial surface of implant

One root-form implant (3.80-mm diameter, 13-mm) with a screw-retained MH-6 abutment (Frios, Frialit; Friadent GmbH, Mannheim, Germany) was used as the investigated implant system. The implant (Frios, Frialit) was placed in the second molar region, and modeling of the implant and the supporting components was performed according to information provided by the manufacturer.

Conventional preparation techniques were applied for the preparation of natural teeth and creation of metal ceramic restorations.[38] Ni-Cr alloy was used as a metal substructure material. In designs where the attachment was placed on the tooth, heavier preparation was required to accommodate the attachment. A slide-type attachment (T-123; Metalor, Neuchatel, Switzerland) indicated for a fixed prosthesis was used as the NRC. The vertical length of the NRC was fixed as 5 mm for all FEA models. The interfacial frictional surface (contact elements) was modeled to simulate the adaptation between the matrix and patrix components of the NRC to more realistically simulate the compensative mechanism within the sliding function of NRC. It allowed the nodes to slide in the tangential direction without penetration between different materials. A value of 0.5 was considered as the friction coefficient for all contact surfaces.

The models were created (Bias Electronics; Mechanical, Computer, Engineering, Consulting, Inc., Ankara, Turkey) using an FEA Program (Marc K7.2/Mentat 2001). The materials used for the models were evaluated as homogenous, isotropic, and linear, and the implants directly in contact with the bone were assumed to be completely osseointegrated. All models had, on average, 10,500 nodes and 5130 elements. The nodes at the surfaces of the alveolar bone in the FEMs were fixed in all directions as the boundary condition. The elasticity modulus (E) of materials used in the study and their Poisson's ratio (v) are determined from the literature and presented in Table 2.

Prepared 2D solid mathematical models were divided into triangular elements, and linear static analysis was performed. Occlusal loads of 50 N static vertical (0° to the long axis of supports) and oblique (30° to the long axis of supports) were

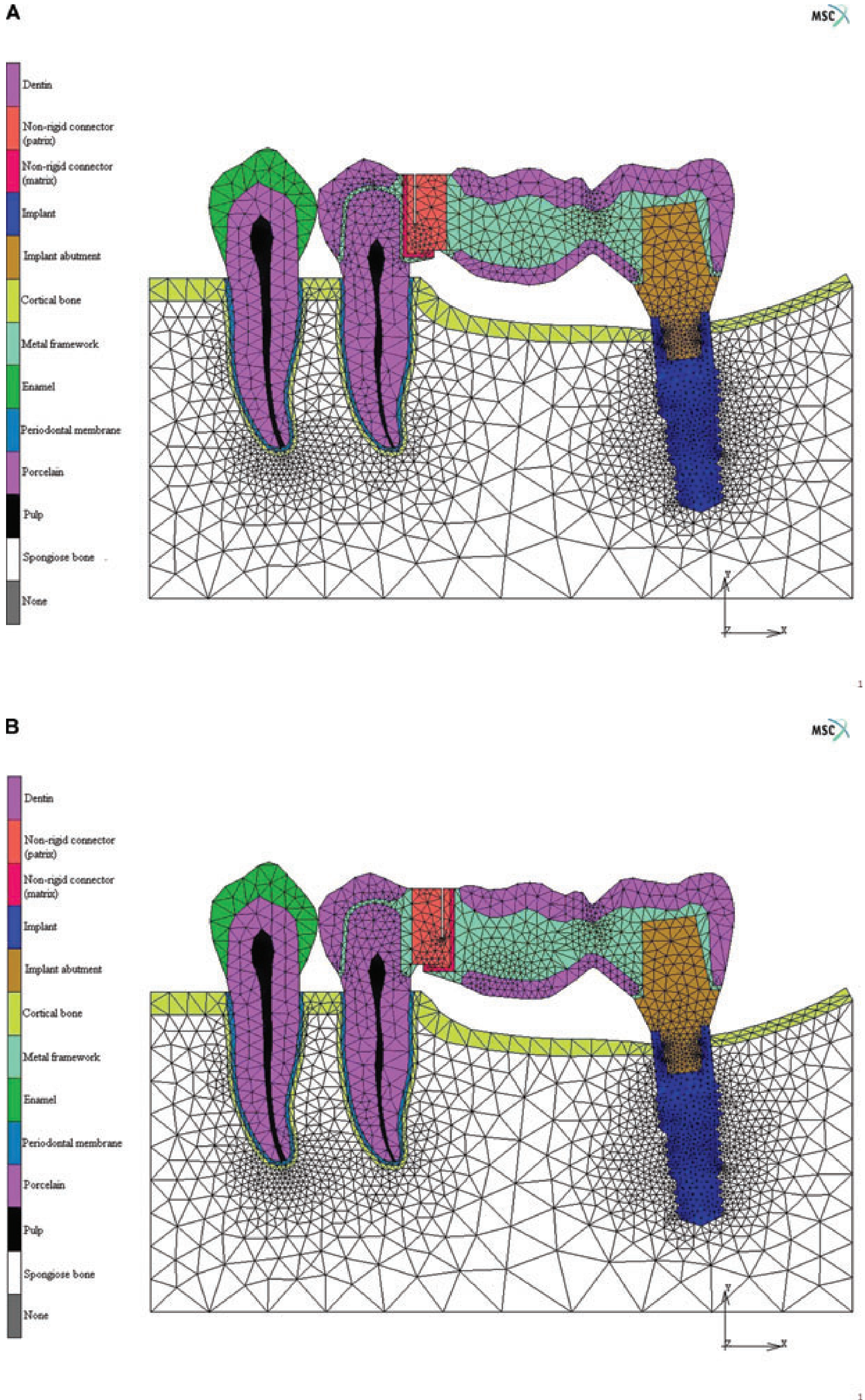

Figure 1 (A) *Model MDP*: The second premolar and the implant connected by nonrigid connector with matrix positioned on distal surface of second premolar. (B) *Model PDP:* The second premolar and implant connected by nonrigid connector with patrix positioned on distal surface of

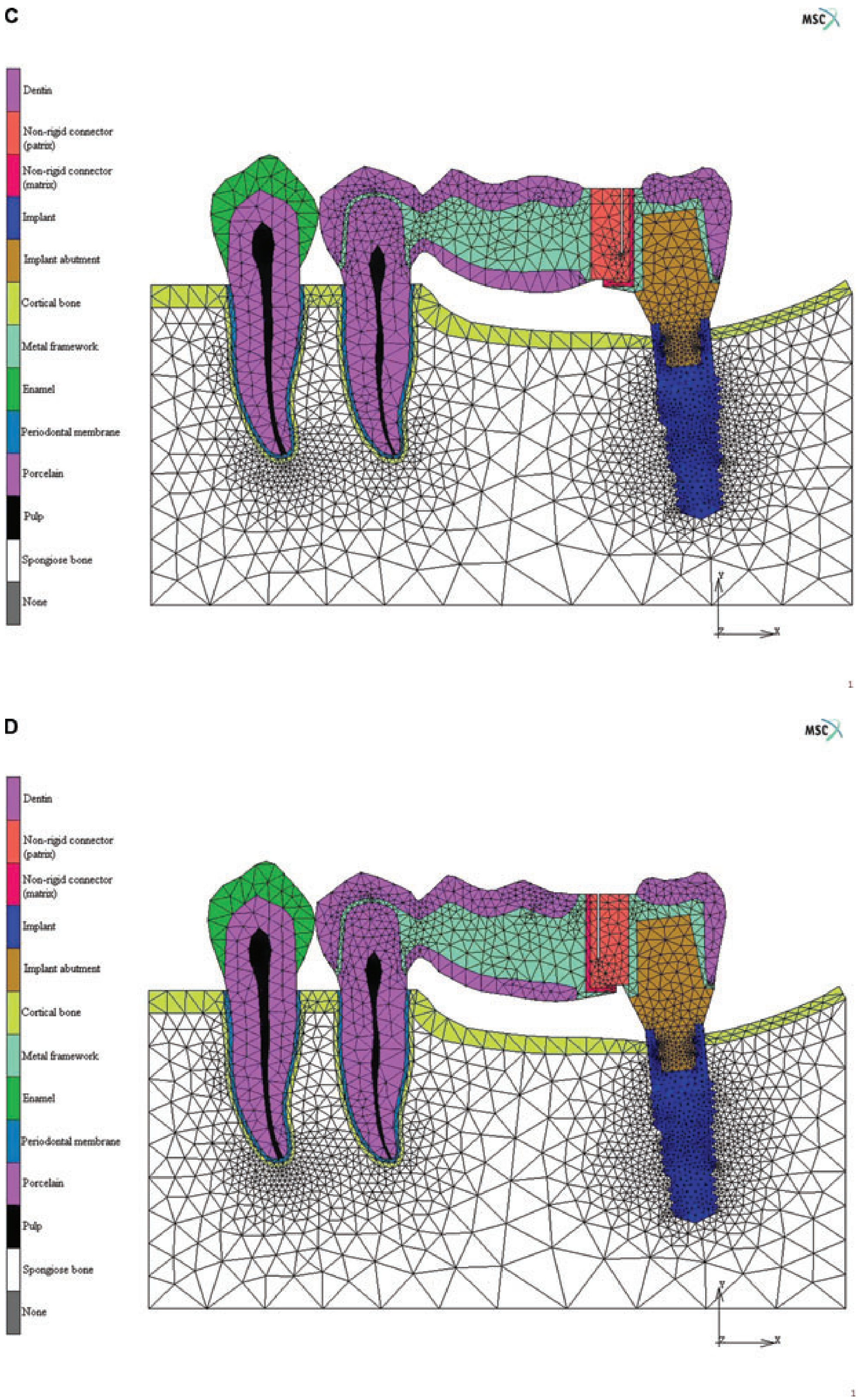

Figure 1 (Continued) second premolar. (C) *Model MMI:* The second premolar and implant connected by nonrigid connector with matrix positioned on mesial surface of implant. (D) *Model PMI:* The second premolar and implant connected by nonrigid connector with patrix positioned on mesial surface of implant.

Table 2 Materials' elasticity modulus (E) and Poisson's ratio (v)

Material properties	Elasticity modulus (E) (GPa)	Poison proportion (v)
Dentin[39]	18.6	0.31
Implant[40]	110	0.33
Cortical bone[40]	15	0.30
Ni-Cr alloy[41]	218	0.33
Enamel[42]	84	0.33
Periodontal membrane[43]	2	0.45
Porcelain[39]	69	0.28
Pulp[44]	0.002	0.45
Spongiose bone[40]	1.5	0.30
Nonrigid attachment	110	0.33

applied on each cusp to calculate the stress distributions (Fig 2). The maximum equivalent Von Mises (VM_{Max}), which is the total value of the pressure, the tensile, and the shear tensions, was evaluated for each model on six lines. The VM_{Max} values obtained from each plane on 2D FEA models were presented in tables. Afterwards, calculated numeric data were transformed into color graphics to better visualize the mechanical phenomena in the models.

Results

Model MDP (the second premolar and the implant are connected by an NRC with the matrix positioned on the distal side of the second premolar): The peak stress values were located at the cortical bone region of the implant along Lines 5 and 6. The highest VM_{Max} value occurred at Line 5 (60.309 MPa), which represented the mesial crestal region of the implant/bone interface when load at a right angle was applied (Fig 3A). When a force 30° to the long axis of the supports was applied, the highest VM_{Max} value occurred at Line 4 (74.45 MPa), representing the distal connector area (Fig 3B).

Model PDP (the second premolar and the implant are connected by an NRC with the patrix positioned on the distal side of the second premolar): The maximum VM_{Max} values were obtained on the cortical bone region of both the distal and the mesial sides along Lines 5 and 6 with values ranging between 50.176 and 30.613 MPa, respectively. The highest VM_{Max} value was observed at Line 5 (50.176 MPa), representing the mesial

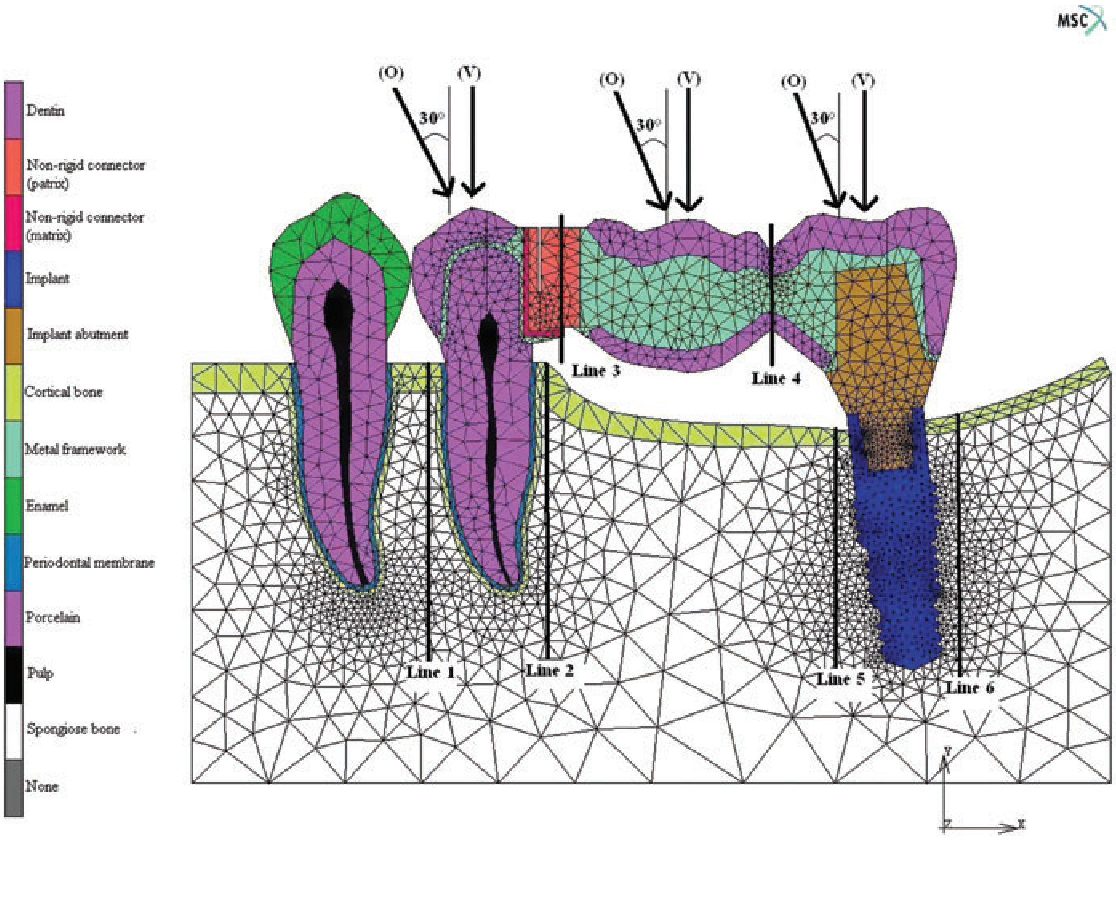

Figure 2 Direction of applied (V) vertical and (O) oblique occlusal loads. Maximum equivalent Von Mises (VM_{Max}) on surface of bone adjacent to natural tooth/implant and connector areas was evaluated on six lines.

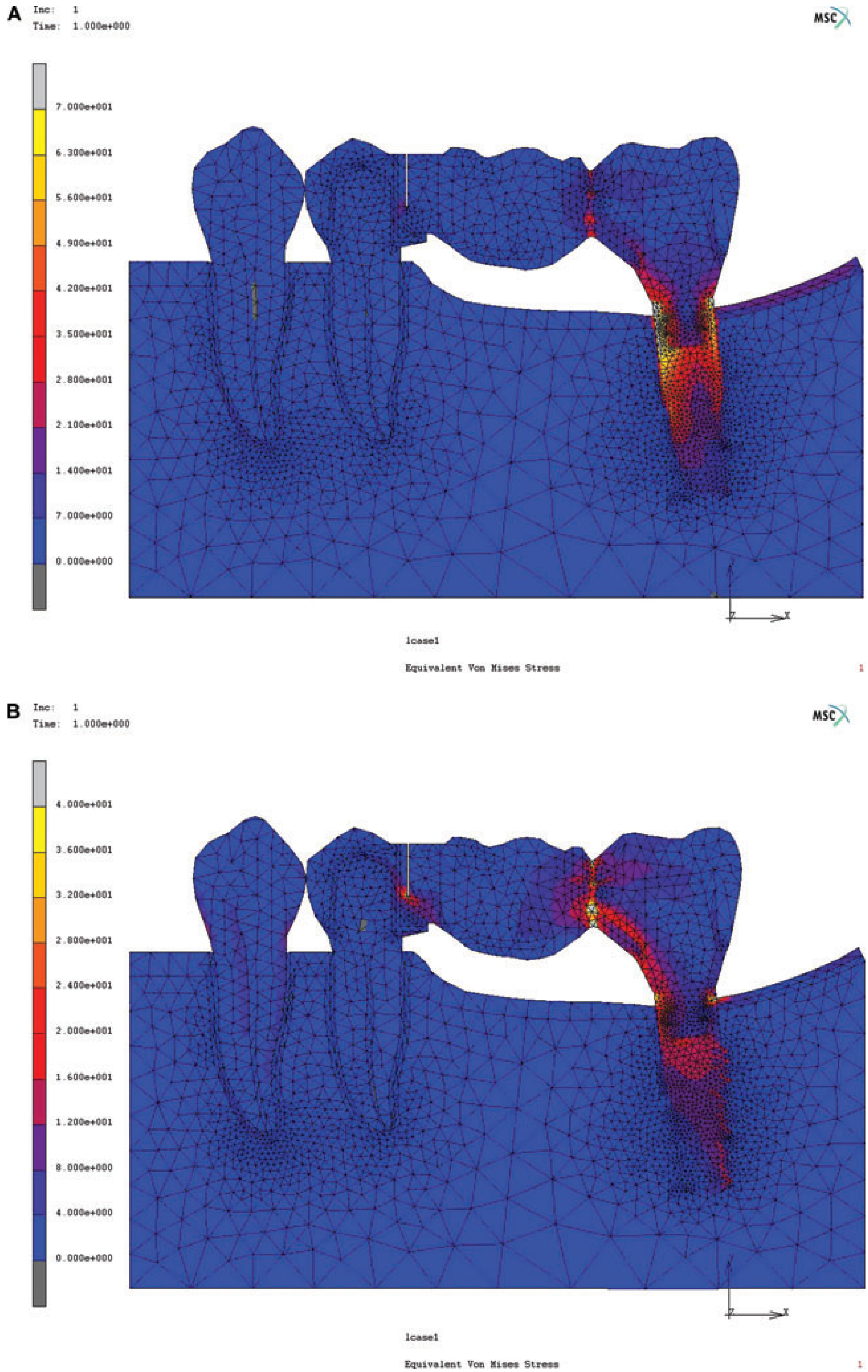

Figure 3 (A) Stress distribution in 2D FEA Model MDP under vertical occlusal loads. (B) Stress distribution in 2D FEA Model MDP under oblique occlusal loads.

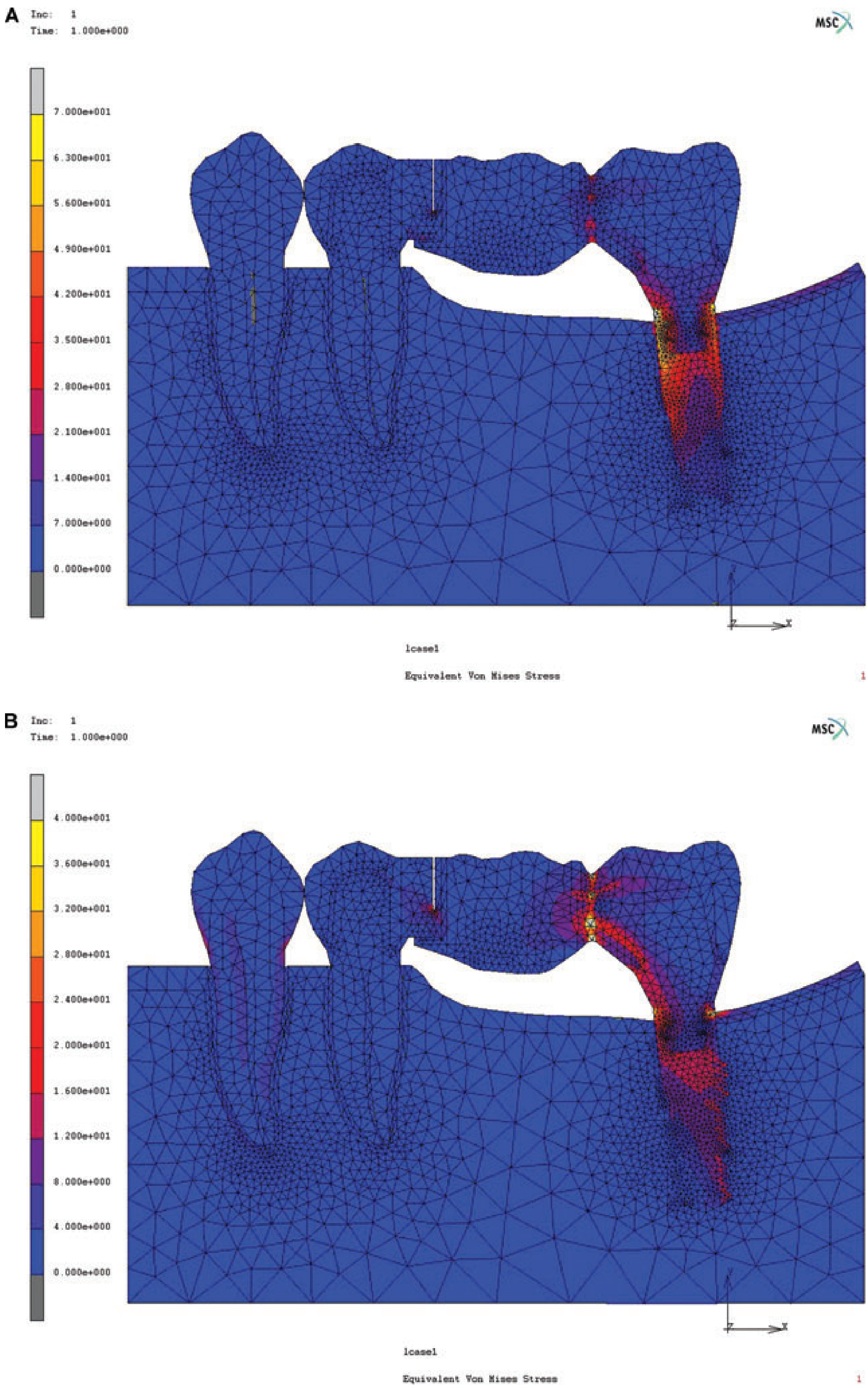

Figure 4 (A) Stress distribution in 2D FEA Model PDP under vertical occlusal loads. (B) Stress distribution in 2D FEA Model PDP under oblique occlusal loads.

crestal region of the implant/bone interface when load at a right angle was applied (Fig 4A). When a force 30° to the long axis of the supports was applied, the highest VM_{Max} value occurred at Line 4 (392.8 MPa), representing the distal connector area (Fig 4B).

Model MMI (the second premolar and the implant are connected by an NRC with the matrix connector positioned on the mesial side of the implant): The highest VM_{Max} stress values were 30.644 and 20.183 MPa, and these values were located on the cortical region of the implant abutment along Lines 5 and 6 (Fig 5A). When a force 30° to the long axis of the supports was applied, the highest VM_{Max} value occurred at Line 4 (66.58 MPa), which represented the distal connector area (Fig 5B).

Model PMI (the second premolar and the implant are connected by an NRC with the patrix positioned on the mesial side of the implant): The highest VM_{Max} value occurred at Line 4 (200.289 MPa), representing the distal connector area when load at right angle was applied (Fig 6A). When a force 30° to the long axis of the supports was applied, the peak VM_{Max} value occurred at Line 4 (313.4 MPa), representing the distal connector area (Fig 6B).

VM_{Max} values on selected critical regions of the models are summarized in Tables 3 and 4.

Discussion

The most important factor for long-term success of a TIFP is the biomechanical aspect of the restoration. Research and clinical observation do not provide sufficient information to determine the biomechanics for a complex TIFP. FEA models have had widespread use in dentistry in biomechanics of stress transfer studies[28,31–36]; however, the 2D FEA program used in this research has several limitations in regard to the simulation of material properties of the structure.

The authors accept the bone, the tooth, and the periodontal ligament as homogeneous, linear-elastic, and isotropic, and the osseointegration of the implant as perfect. In reality, the mastication forces are dynamic and oblique relative to the occlusal surface of TIFPs, and the relation between the implant and the bone is dynamic; however, in this study, all masticatory forces applied to fixed prostheses were static and were 0° (vertical) and 30° (oblique) to the long axis of the supports. Consequently, in such biomechanical studies, it is usually not possible to reproduce the intraoral situation. Thus, the data obtained in this study may not resemble actual values, yet, at most, these may show varying stress distribution differences among different models and which TIFP design is more advantageous. Besides, this method provides visual and quantifiable information for interpretation.

Three-dimensional FEA has previously been used in biomechanical stress distribution investigations[28,31,33,34,36]; however, the 3D FEA model for bio-structure is relatively difficult to construct, especially in complicated three- or four-unit prosthesis/abutment teeth systems and expensive when compared to 2D FEA. A 2D FEA model may simulate the complicated problem in a qualitatively reasonable manner and help to understand the tendency of mechanical behaviors; however, in the 2D system, it is assumed that out-of-plane deformations, strains, and stresses are negligible. This may reduce the cost of analysis, but it also introduces more error due to the assumed artificial boundary conditions. Three-dimensional models may provide more realistic results[28,31,33,34,36]; however, to date, the 2D FEA has been used when numerous, varied models, and designs are evaluated in the literature.[32,33,35] As many models and designs were analyzed in this study, 2D FEA was chosen based on practical considerations; however, this kind of 2D FEM study outcome might be supported with the results obtained from strain gauge stress analysis technique in future studies. This might be also considered a limitation of this study.

The stress distribution patterns under vertical occlusal and oblique occlusal loads applied in the present study were different for implant and teeth in all 2D FEMs as reported in previous studies.[28,31–36] The stress distribution values of natural tooth were relatively more uniform than that of the implant. The stress distribution opposite to applied (vertical and oblique) forces was transmitted to the bone along the long axis of the implant, and the distribution was intensive in the cervical area of the implant neck. This was particularly evident up to the 7th and 8th grooves of the implant decreased apically; however, the stress values of the natural tooth increased from the cervical region toward the apical area, which is considered to be the ideal direction to minimize bone resorption, and the values were relatively lower than that of the implant. The different stress distribution patterns obtained from the implant and natural tooth may be attributed to the periodontal ligament's load-absorbing feature against occlusal stresses, which does not exist for an implant.

Another possible reason for maximum stress formation in the cervical region of implant support may be due to the two structures of alveolar bone (cortical and spongious), which have different elastic moduli. This phenomenon relies on the presence of cortical bone, which has higher elastic modulus, at the surface.

In this study, under a vertical occlusal load, stress increase occurred on the mesio-cervical surface of the implants with all TIFP designs. Because the implants were assumed to be 100% integrated, the movement of the implants in bone is at the micron level. The applied static vertical occlusal loads intrude the natural tooth into the alveolus and may cause stresses in the mesio-cervical regions of the implant due to the bending moment that occurred. These bending moments force the implant to rotate, and because the center of rotation of the implant at the crestal bone level is higher compared to natural teeth, stress accumulation occurs in the cortical bone area. Another reason stresses accumulate in this area may be the presence of cortical bone with a higher elastic modulus on the outer bone surface, as previously mentioned.[2,4–10]

Therefore, these bending moments result in overload on implants, particularly in natural tooth/implant restoration designs. These bending moments occur in fixed partial restorations with three-unit linear prosthetic designs as conducted in the present study. Therefore, these bending forces should be considered when fabricating restorations.

When the 2D FEA models were evaluated in regard to the 30° mesio-oblique occlusal load applied along the axis of the implant and tooth, stress distribution exhibited differences in support when compared with vertical occlusal loading. The stresses were observed to accumulate along the distal surfaces

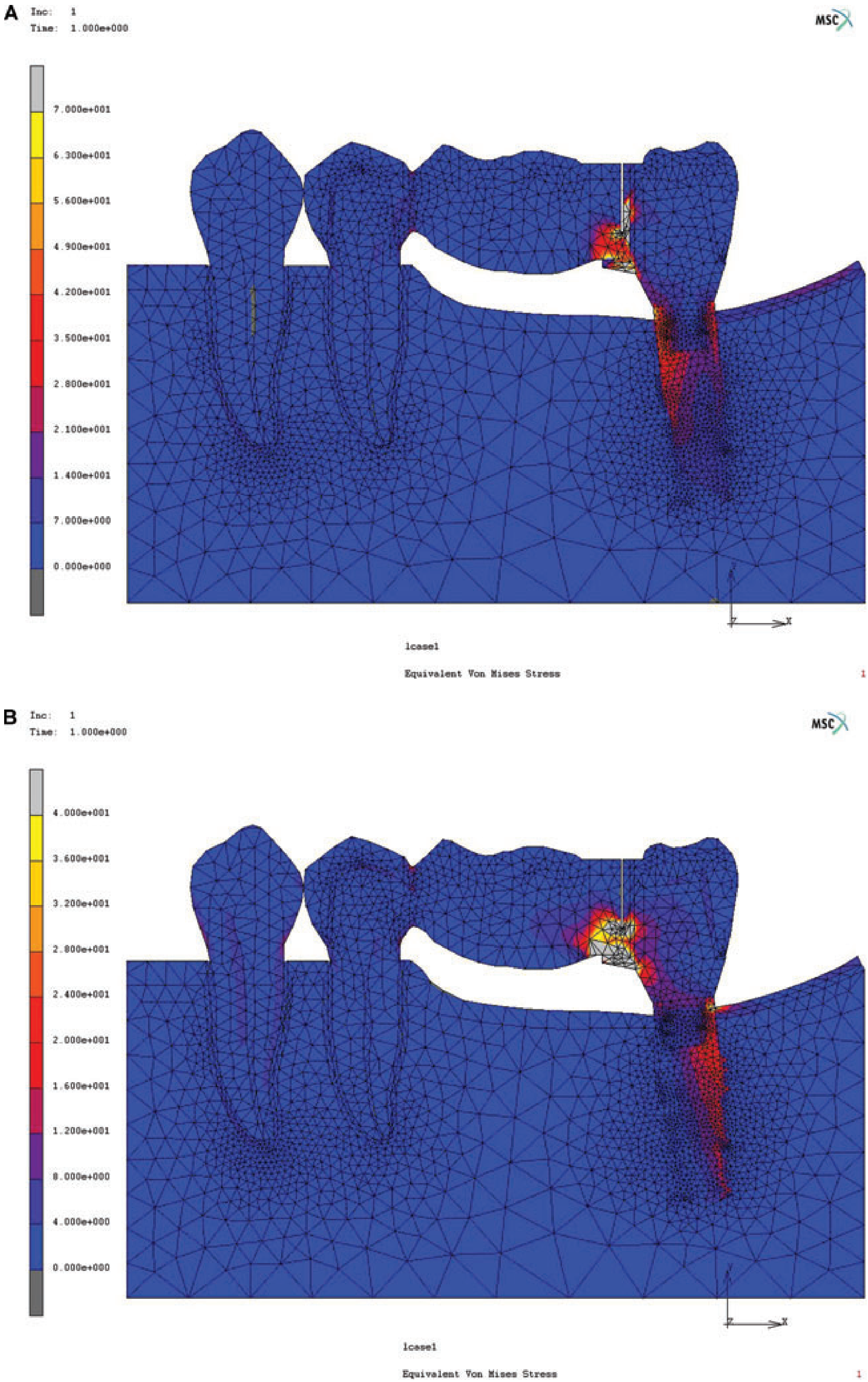

Figure 5 (A) Stress distribution in 2D FEA Model MMI under vertical occlusal loads. (B) Stress distribution in 2D FEA Model MMI under oblique occlusal loads.

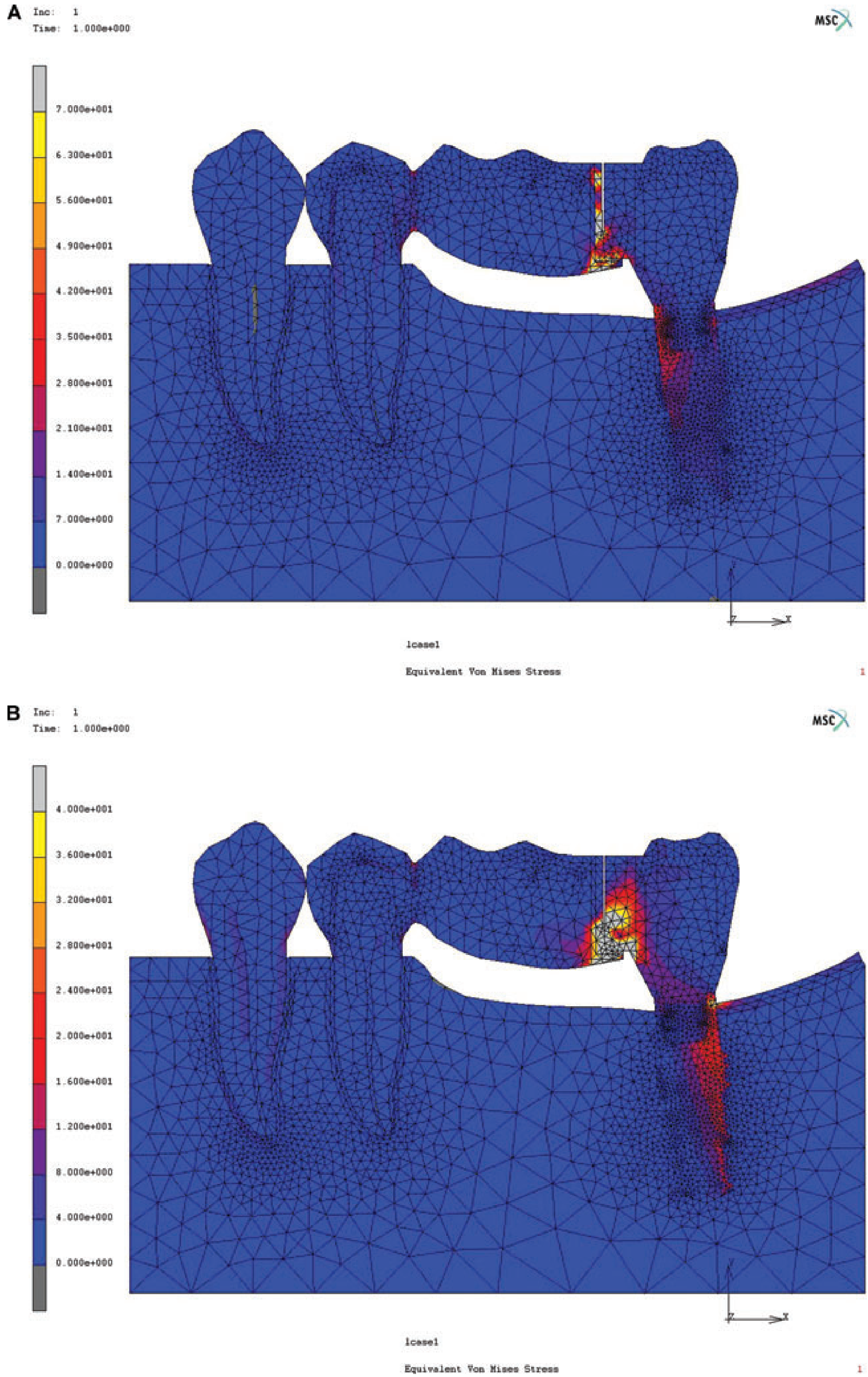

Figure 6 (A) Stress distribution in 2D FEA Model PMI under vertical occlusal loads. (B) Stress distribution in 2D FEA Model PMI under oblique occlusal loads.

Table 3 Maximum equivalent Von Mises (VM_{Max}) (MPa) at critical regions with vertical occlusal loading of 2D FEA models

	Natural tooth		Connector areas		Implant abutment	
	Line 1	Line 2	Line 3	Line 4	Line 5	Line 6
Model MDP	2.182	3.488	30.052	60.14	60.309	40.543
Model PDP	2.601	2.880	40.962	50.159	50.176	30.613
Model MMI	3.222	3.561	20.786	400.377	30.644	20.183
Model PMI	3.317	3.539	30.461	200.289	20.658	10.517

Table 4 Maximum equivalent Von Mises (VM_{Max}) (MPa) at critical regions with 30° oblique loading of 2D FEA models

	Natural tooth		Connector areas		Implant abutment	
	Line 1	Line 2	Line 3	Line 4	Line 5	Line 6
Model MDP	1.596	8.258	69.23	74.45	12.31	23.14
Model PDP	2.346	7.08	40.18	66.58	10.56	23.8
Model MMI	2.521	8.245	19.54	392.8	5.636	27.6
Model PMI	2.496	7.679	18.22	313.4	5.407	27.88

of both the natural tooth and implant. Stress distribution on the natural tooth increased from the cervical toward the apical area, whereas decreased stress was observed in the same direction on the implant, as was mentioned after vertical occlusal loading. When the transmission of the stresses to bone was considered, in all 2D FEA models, the highest VM_{Max} values occurred with the 30° mesio-oblique occlusal load at the distal cortical bone region of the implant.

In this study, the areas of stress concentration were the connectors and NRCs, depending on the applied vertical occlusal and oblique occlusal loads. In models MDP and PDP, where an NRC was used close to the natural tooth, there were minor differences found between the two distinct connection areas in terms of stress concentration; however, in models MMI and PMI, where the NRC was placed close to the implant site, the stress concentrated near the bottom contact areas of the keyway device, and the VM_{Max} values increased to over 400 MPa.

When models MMI and PMI were compared, the stress concentration on the NRC in model MMI was twice the value of that in model PMI. Furthermore, the stress concentration in the connector site close to the natural tooth was 15% more in model PMI than in model MMI. In the authors' opinion, the high stress concentration values on NRC revealed that the NRC accomplished its goal of breaking the stresses; however, this stress accumulation on the NRC is considered to be unfavorable and may result in failure of the prostheses by deformation of the NRC in clinical use after long-term dynamic loads. Theoretically, the attachment at the connector could be open (the displacement of the attachment move to mesial and distal). This phenomenon is very important and is the main problem for the slide-type attachments. Lin et al[33] noted the same issue in their studies. Stress accumulation on the NRC may be attributed to the 2D character of the designs and is only applicable for the NRC used in the present study.

Therefore, the 2D FEA modeling results provide only a general insight into the biomechanical aspects of the TIFPs under controlled conditions. To better simulate the complexities of the clinical environment, further in vivo and in vitro studies are needed to better understand the biomechanical behavior of TIFP.

When all the models are considered in terms of stress formation around both the implant and natural tooth under occlusal loads, model MMI and PMI were found to be the favorable options, where the NRC was positioned close to the implant site. Furthermore, model PMI, where the patrix of the NRC was placed on the implant site, demonstrated better stress distribution results than model MMI. Consequently, use of the NRC on the implant site may be more efficient in regard to compensation for the movement disparity between the natural tooth and implant under occlusal loads applied in this study; however, as previously mentioned, the NRC should be used with caution because it breaks the stress transfer and increases the unfavorable stress values at the connector site where the nonrigid attachment was placed.

Conclusions

Within the limitations of this study, the following conclusions were drawn:

(1) Under vertical occlusal loads, in designs where the NRC was placed on the implant, the stress formed around the implant decreased when compared to the designs where the NRCs were positioned on the tooth.
(2) The use of the NRC exhibited varying behavior depending on the direction of the load applied.
(3) The use of the patrix of the NRC on the implant may more effectively reduce stress formation around the implant.
(4) When the NRC is placed on the implant, there may be problems associated with unfavorable stress formation on the NRC.

References

1. Langer B, Sullivan DY: Osseointegration: its impact on the interrelationship of periodontics and restorative dentistry: Part II. Int J Periodontics Restorative Dent 1989;9:165-183
2. Kay HB: Free-standing versus implant-tooth-interconnected restorations: understanding the prosthodontic perspective. Int J Periodontics Restorative Dent 1993;13:47-69
3. Parel SM: Prosthesis design and treatment planning for the partially edentulus implant patient. J Oral Implantol 1996;22:31-33
4. Skalak R: Aspects of biomechanical considerations. In Branemark PI, Zarb GA, Albrektsson T (eds): Tissue-Integrated Prostheses: Osseointegration in Clinical Dentistry. Chicago, Quintessence, 1985, pp. 117-128
5. Skalak R: Osseointegration biomechanics. J Oral Implantol 1986;12:350-356
6. Richter EJ: Basic biomechanics of dental implants in prosthetic dentistry. J Prosthet Dent 1989;61:602-609
7. Weinberg LA, Kruger B: Biomechanical considerations when combining tooth-supported and implant-supported prostheses. Oral Surg Oral Med Oral Pathol 1994;78:22-27
8. Glantz PO, Nilner K: Biomechanical aspects of prosthetic implant-borne reconstructions. Periodontol 2000 1998;17:119-124
9. Lundgren D, Laurell L: Biomechanical aspect of fixed bridgework supported by natural teeth and endosseous implants. Periodontol 2000 1994;4:23-40
10. Cohen SR, Orenstein JH: The use of attachments in combination implant and natural-tooth fixed partial dentures: a technical report. Int J Oral Maxillofac Implants 1994;9: 230-234
11. Cho GC, Chee WW: Apparent intrusion of natural teeth under an implant-supported prosthesis: a clinical report. J Prosthet Dent 1992;68:3-5
12. Bechelli AH: The osseointegrated prosthesis—combination of osseointegrated implants and natural teeth in fixed prostheses. J Oral Implantol 1992;18:62-65
13. Sheets CG, Earthman JC: Tooth intrusion in implantassisted prostheses. J Prosthet Dent 1997;77:39-45
14. Garcia LT, Oesterle LJ: Natural tooth intrusion phenomenon with implants: a survey. Int J Oral Maxillofac Implants 1998;13:227-231
15. Schlumberger TL, Bowley JF, Maze GI: Intrusion phenomenon in combination tooth-implant restorations: a review of the litrature. J Prosthet Dent 1998;80:199-203
16. Naert I, Quirynen M, van Steenberghe D, et al: A six-year prosthodontic study of 509 consecutively inserted implants for the treatment of partial edentulism. J Prosthet Dent 1992;67: 236-245
17. Naert IE, Duyck JA, Hosny MM, et al: Freestanding and tooth-implant connected prostheses in the treatment of partially edentuluous patients. Part II. An up to 15- years radiographic evaluation. Clin Oral Implants Res 2001;12:245-251
18. Pesun IJ: Intrusion of teeth in the combination implant-to-natural-tooth fixed partial denture: a review of the theories. J Prosthodont 1997;6:268-277
19. Lindh T, Gunne J, Danielsson S: Rigid connections between natural teeth and implants: a technical note. Int J Oral Maxillofac Implants 1997;12:674-678
20. Ericsson I, Lekholm U, Brånemark PI, et al: A clinical evaluation of fixed-bridge restorations supported by the combination of teeth and osseointegrated titanium implants. J Clin Periodontol 1986;13:307-312
21. Gunne J, Astrand P, Lindh T, et al: Tooth-implant and implant supported fixed partial dentures: a 10-year report. Int J Prosthodont 1999;12:216-221
22. Rangert B, Gunne J, Glantz PO, et al: Vertical load distribution on a three-unit prosthesis supported by a natural tooth and a single Brånemark implant. An in vivo study. Clin Oral Implants Res 1995;6:40-46
23. Nickenig HJ, Schäfer C, Spiekermann H: Survival and complication rates of combined tooth-implant supported fixed partial dentures. Clin Oral Implants Res 2006;17:506-511
24. Naert IE, Ducky JAJ, Honsy MMF, et al: Freestanding and tooth implant connected prostheses in the treatment of partially edentulous patients. Part I: an up to 15-years clinical evaluation. Clin Oral Implants Res 2001;12:237-244
25. Hosny M, Duyck J, van Steenberghe D, et al: Within-subject comparison between connected and nonconnected tooth-to-implant fixed partial prostheses: up to 14-year follow-up study. Int J Prosthodont 2000;13:340-346
26. Olsson M, Gunne J, Astrand P, et al: Bridges supported by free-standing implants versus bridges supported by tooth and implant. A five-year prospective study. Clin Oral Implants Res 1995;6:114-121
27. Gross M, Laufer BZ: Splinting osseointegrated implants and natural teeth in rehabilitation of partially edentulous patients. Part I: laboratory and clinical studies. J Oral Rehabil 1997;24:863-870
28. Menicucci G, Mossolov A, Mozzati M, et al: Tooth-implant connection: some biomechanical aspects based on finite element analysis. Clin Oral Implants Res 2002;13:334-344
29. Tangerud T, Gronningsater AG, Taylor A: Fixed partial dentures supported by natural teeth and Branemark system implants: a 3-year report. Int J Oral Maxillofac Implants 2002;17:212-219
30. Naert IE, Ducky JAJ, Honsy MMF, et al: Freestanding and tooth-implant connected prostheses in the treatment of partially edentulous patients. Part II: an up to 15-years radiographic evaluation. Clin Oral Implants Res 2001;12:245-251
31. Misch CM, Ismail YH: Finite element stress analysis of tooth-to-implant fixed partial denture designs. J Prosthodont 1993;2:83-92
32. Melo C, Matsushita Y, Koyano K, et al: Comparative stress analyses of fixed free-end osseointegrated prostheses using the finite element method. J Oral Implantol 1995;21:290-294
33. Lin CL, Chang SH, Wang JC, et al: Mechanical interactions of an implant/tooth-supported system under different periodontal supports and number of splinted teeth with rigid and non-rigid connections. J Dent 2006;34:682-691
34. Lin CL, Wang JC, Chang WJ: Biomechanical interactions in tooth-implant-supported fixed partial dentures with variations in the number of splinted teeth and connector type: a finite element analysis. Clin Oral Implants Res 2008;19:107-117
35. Ozçelik T, Ersoy AE: An investigation of tooth/implant-supported fixed prosthesis designs with two different stress analysis methods: an in vitro study. J Prosthodont 2007;16:107-116
36. Oruc S, Eraslan O, Tukay HA, et al: Stress analysis of effects of non-rigid connectors on fixed partial dentures with pier abutments. J Prosthet Dent 2008;99:185-192
37. Wheeler RC: Dental Anatomy, Physiology and Occlusion (ed 5). Philadelphia, Saunders, 1974
38. Shillingburg HT, Hobo S, Whitsett LD, et al: Fundamentals of Fixed Prosthodontics (ed 3). Chicago, Quintessence, 1997, pp. 455-483
39. Holmes DC, Diaz-Arnold AM, Leary JM. Influence of post dimension on stress distribution in dentin. J Prosthet Dent 1996;75:140-147

40. Holmgren EP, Seckinger RJ, Kilgren LM, et al: Evaluating parameters of osseointegrated dental implants using finite element analysis-a two-dimensional comparative study examining the effects of implant diameter, implant shape, and load direction. J Oral Implantol 1998;24:80-88
41. Sertgöz A: Finite element analysis study of the effect of superstructure material on stress distribution in an implant-supported fixed prosthesis. Int J Prosthodont 1997;10:19-27
42. Kamposiora P, Papavasilious G, Bayne SC, et al: Finite element analysis estimates of cement microfracture under complete veneer crowns. J Prosthet Dent 1994;71:435-441
43. van Rossen IP, Braak LH, de Putter C, et al: Stress-absorbing elements in dental implants. J Prosthet Dent 1990;64: 198-205
44. O'Grady J, Sheriff M, Likeman P: A finite element analysis of a mandibular canine as a denture abutment. Eur J Prosthodont Restor Dent 1996;4:117-121